



## DISCRETE-DIFFERENTIAL MODELLING OF BIOFILM STRUCTURE

C. Picioreanu<sup>\*\*\*</sup>, M. C. M. van Loosdrecht<sup>\*</sup> and  
J. J. Heijnen<sup>\*</sup>

<sup>\*</sup> Department of Biochemical Engineering, Delft University of Technology,  
Julianalaan 67, 2628 BC Delft, The Netherlands

<sup>\*\*</sup> Department of Chemical Engineering, University Politehnica of Bucharest,  
Splaiul Independentei 313, 77206 Bucharest, Romania

### ABSTRACT

A fully quantitative two- and three-dimensional approach for biofilm growth and structure formation has been developed. The present model incorporates the flow over the irregular biofilm surface, convective and diffusive mass transfer of substrate, bacterial growth and biomass spreading. A future model will also include a mechanism for biofilm detachment due to biofilm deformation stress. Any arbitrary shape of the carrier surface can be accommodated in the model, as well as multispecies and multisubstrate biofilms. Results of model simulations show that the ratio between nutrient transfer rate to the biofilm and the bacterial growth rate influences to a great extent the biofilm roughness and porosity. A low mass transfer rate, i.e., low Reynolds numbers or high values of Thiele modulus, results in the development of a rough and open biofilm. When the biofilm growth is not limited by the substrate availability but by the rate of bacterial metabolism, the biofilm forms as a compact and homogeneous structure. The multidimensional biofilm modelling approach we used is very suitable for theoretical investigation of factors that affect biofilm structure and ecology. © 1999 IAWQ Published by Elsevier Science Ltd. All rights reserved

### KEYWORDS

Biofilm; multidimensional modelling; structure; roughness; porosity; flow; convection; diffusion.

### INTRODUCTION

Research done in past years shows that biofilms develop in a multitude of patterns (Kugaprasatham *et al.* 1992; Gjaltema *et al.*, 1994). Traditionally, development of biofilms was seen as the formation of a layered structure growing from the substratum up. This led to the, now traditional, one-dimensional models (for example, Wanner and Gujer, 1986; Rittmann and Manem, 1992). All the property gradients (like those of substrate concentration, biomass density, porosity, etc.) are one-dimensional, varying only in the direction from the bulk liquid to the carrier surface. There is, however, significant spatial variability in biofilm density, porosity, surface shape, microbial activity and distribution in clusters (Gjaltema *et al.*, 1994; de Beer *et al.*, 1994; de Beer and Stoodley, 1995; Wentland *et al.*, 1996). Bishop and Rittmann (1996) suggested that while one-dimensional models can be adequate for description alone, multidimensional modelling may be required for prediction of biofilm heterogeneity. In a model that should predict biofilm structural properties such as surface shape, porosity, pore and channel sizes, these same properties must be not only the output of the model but they are also the boundary conditions which change in time.

Modelling the structural development of a biofilm is a great challenge because of the complex interaction between many processes. The biofilm development is determined by “positive” processes, like cell attachment, cell division, and polymer production, which lead to biofilm volume expansion, and “negative” processes, like cell detachment and cell death, which contribute to biofilm shrinking. By changing the balance between these two types of processes, biofilms with different structural properties like porosity, compactness or surface roughness can be formed, as was hypothesised by van Loosdrecht *et al.* (1995) and experimentally shown by Kwok *et al.* (1998).

The main biofilm expansion is due to bacterial growth and to extracellular polymers produced. The nutrients necessary for bacterial growth are dissolved in the liquid flow and to reach the cells they pass first through the boundary layer (external mass transfer) and then through the biofilm matrix (internal mass transfer). The external mass transfer resistance is given by the thickness of the concentration boundary layer (CBL), which is directly correlated to the hydrodynamic boundary layer (HBL) resulting from the flow pattern over the biofilm surface. We can therefore say that on one hand the fluid flow drives the biofilm growth by regulating the concentration of substrates and products at the liquid-solid interface. On the other hand, the flow shears the biofilm surface, eroding the protuberances. While the flow changes the biofilm surface, the interaction is reciprocal because a new biofilm shape leads to a different boundary condition thus different flow and concentration fields. This leads further to the concept of temporal heterogeneity: the biofilm is a dynamic structure evolving in nonsteady-state conditions. However, as we will see later, due to the very different magnitude of process time constants, for practical computational reasons it can be assumed that some processes are at equilibrium while others are in a dynamic or frozen regime.

For a biofilm model capable of full description of the three-dimensional heterogeneity it is of importance that the model can easily cope with a large variation in time constants and with continuously changing boundary conditions. With this in mind, we started to develop a model based on a discrete algorithm (a cellular automaton approach, Picioreanu, 1996, Picioreanu *et al.*, 1998a,b). Similar approaches have been reported also by Wimpenny and Colasanti (1997) and Hermanowicz (1998), but despite the fact that their models generate biofilms with qualitative features somehow resembling the real ones, their models work in a completely abstract time and space. There is no direct link between their model parameters and the real values of some widely accepted parameters such as diffusivities, reaction rate constants, etc. Moreover, we found that for some of the processes a traditional differential approach could be more advantageous (Picioreanu *et al.*, 1998a,b). This led to a combined discrete-differential model for the formation of biofilms. Below, the general structure of this model is described together with a few model applications.

### MODEL EQUATIONS

The equations describing the biofilm system in unsteady-state are:

- total mass conservation for the fluid phase (the continuity equation):

$$\nabla \cdot \mathbf{u} = 0 \quad (1)$$

- momentum conservation for the fluid phase flowing around the biofilm (the Navier–Stokes equations):

$$\frac{\partial \mathbf{u}}{\partial t} + \mathbf{u} \cdot \nabla \mathbf{u} = -\frac{1}{\rho} \nabla p + \nu \nabla^2 \mathbf{u} \quad (2)$$

- mass conservation for one dissolved component (for the limiting substrate only):

$$\frac{\partial C_S}{\partial t} + \mathbf{u} \cdot \nabla C_S = -R_S(C_S, C_X) + D \nabla^2 C_S \quad (3)$$

- a kinetic equation for biomass growth:

$$\frac{dC_X}{dt} = R_X(C_S, C_X) \quad (4)$$

where  $\mathbf{u}$  is the velocity vector,  $p$  is the pressure,  $\rho$  is the liquid density,  $\nu$  is the liquid kinematic viscosity,  $D$  is the substrate diffusion coefficient,  $R_S$  and  $R_X$  are the rates of substrate consumption and biomass formation, where  $C_S$  and  $C_X$  are the concentration of substrate and biomass, respectively.

## SOLUTION ALGORITHM

The order of magnitude of time constants for convective and molecular transport, biomass growth, biomass decay and detachment can easily be calculated. By assuming, for example, a biofilm characteristic thickness of 0.5 mm, diffusion coefficients in the range  $D=10^{-9}$ - $10^{-10}$  m<sup>2</sup>/s, liquid viscosity  $\nu=10^{-6}$ - $10^{-7}$  m<sup>2</sup>/s, biomass specific growth rate of  $\mu=0.01$ - $0.2$  h<sup>-1</sup>, biomass specific decay rate  $k_d=0.1$ - $1$  day<sup>-1</sup>, detachment rate  $k_{det}=0.001$ - $0.1$  h<sup>-1</sup> and a fluid mean velocity  $u_x=0.001$ - $0.1$  m/s, the time constants are shown in Figure 1.

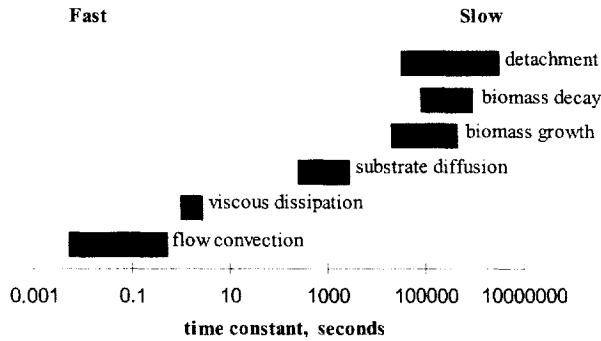


Figure 1. Timescale analysis of biofilm processes.

It can be seen from Figure 1 that biomass growth and detachment rates are much slower than the rate of diffusion of substrate in the biofilm. Also, momentum transport (by convection or dissipation) is much faster than diffusive mass transfer. If the dynamic (nonsteady-state) balance equations for momentum, mass and biomass growth are solved with the smallest time-step, given in this case by the momentum equations, the computational effort needed to obtain the solution of substrate and biomass balances would be far too large. To achieve reduction in complexity, the timescale analysis can be very useful. For instance, while solving the mass balance equation, the flow can be considered at pseudo-equilibrium for a given biofilm shape, and at the same time the biomass growth, decay and detachment are frozen processes. This leads to the idea to use the following strategy in following the biofilm development in time (Figure 2):

1. First, a hydrodynamic step is performed. Momentum transfer and continuity equations are solved to find the flow field variables: pressure  $p$ , velocities  $\mathbf{u}$ , and the normal and tangential stresses  $\tau$  acting on the biofilm surface. This step is needed each time the geometry of the system has changed, for instance by growth (a positive development) or detachment (negative development). Because the time constant of hydrodynamics is much smaller than that of mass transport, the flow will be considered completely established (pseudosteady-state) when the mass transfer calculations are executed.

2. The second step uses the just calculated flow velocities  $\mathbf{u}$  in solving the convective-diffusive mass transfer of soluble components (substrates, products). Mass balance equation is solved towards a pseudosteady-state concentration of substrate,  $C_s$ . The substrate concentration in its turn will be used in the biomass growth kinetic equation. We are allowed to do this because the time constant of growth process is around  $10^5$  s, very slow compared to the substrate mass transfer (especially the diffusive one). Both the first and second step of the model algorithm were performed using a lattice Boltzmann algorithm (Ponce Dawson *et al.*, 1993; Chen *et al.*, 1995; Chen *et al.*, 1997). In the absence of convection however, we preferred a finite-difference algorithm for solving the diffusion-reaction mass balance of substrate (Picioreanu *et al.*, 1998a).

3. The new biomass content of each grid element,  $C_x$ , is calculated by using the Monod and Herbert-Pirt equation including the substrate concentration at steady-state calculated before.

4. As biomass is growing, it has to be redistributed in space according to discrete (cellular automata) rules as used before in Picioreanu *et al.* (1998a,b): by splitting the biomass content in the element in which it has grown above the maximum biomass density, and then by pushing the neighbours to reach the free space.

This competition for space and for substrate generates the biofilm structure. On the other hand this structure determines the further development of the biofilm by changing the flow behaviour and the nutrients/products transport.

5. A detachment step can also be performed before redistribution, because the detachment time constant falls in the same range as the growth time constant ( $10^5$  s). Perhaps this is the reason why biofilm structure is determined by the balance between a positive process, growth, and negative ones such as detachment and decay. If positive and negative terms in this balance have very different values, the biofilm will either infinitely develop (growth not balanced by detachment) or not at all (detachment dominates growth). By using a traditional finite-element method we can compute the deformation energy in the biofilm, induced by the fluid stresses at the biofilm surface. In this way we can determine where the biofilm will break. After the biofilm has lost some biomass, the external structure changes again and a new hydrodynamic step is necessary.

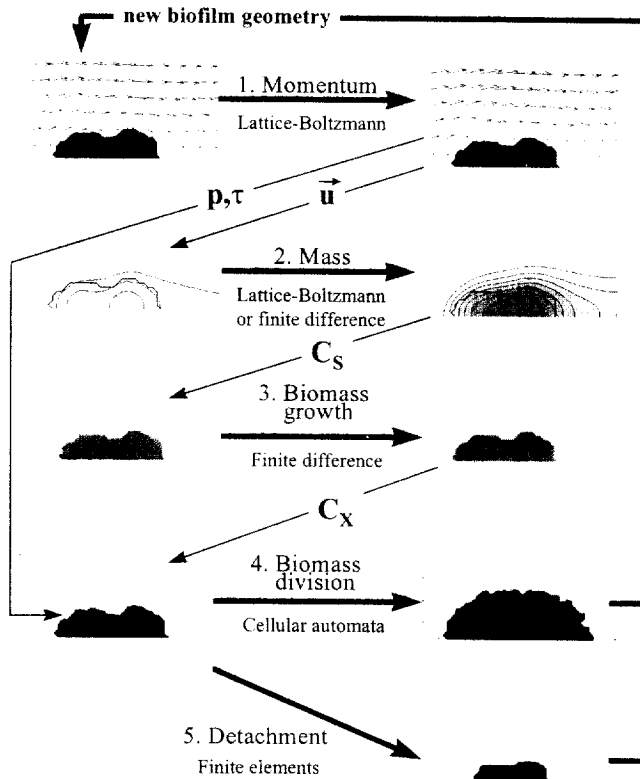


Figure 2. General algorithm used to solve the dynamic biofilm model

## MODEL APPLICATIONS

Results of the model applied for a few particular cases are presented below. A simplified version of the model (DRG model) including only step 2 - Diffusional mass transfer of substrate - together with step 3 - substrate conversion (Reaction) to biomass - and step 4 - biomass Growth - runs both in a 2-D and 3-D space. The number of grid nodes is limited to  $8 \cdot 10^6$  grid nodes (a  $200^3$  cube). An extension of this model, which also includes flow calculation around the biofilm structure (step 1), takes into account convective and diffusive substrate transfer, reaction, and biomass growth (CDRG model). This model is limited to 2-D calculations on maximum  $10^6$  grid nodes on a computer with 128 Mb memory. The full 2-D model including detachment by erosion and sloughing (CDRGD model), is still being tested and its results will be presented in future.

The development of a nitrifying biofilm under oxygen limiting conditions was studied. The biomass growth and substrate uptake kinetics used are presented in Picioreanu *et al.* (1998a,b) and the model parameters are shown in Table 1.

Table 1. Parameters used in the biofilm model

Model parameter	Symbol	Parameter value		Units
		DRG-3D	CDRG-2D	
Computational grid dimensions	$N_x \times N_y \times N_z$	100×100×80	200×200	-
Physical system dimensions	$L_x \times L_y \times L_z$	400×400×320	1000×1000	$\mu\text{m}$
Bulk oxygen concentration	$C_{S0}$	$10^{-2}$ and $0.5 \cdot 10^{-3}$	$4 \cdot 10^{-3}$	$\text{kgX m}^{-3}$
Biomass maximum specific growth rate	$\mu_m$	$1.5 \cdot 10^{-5}$	$1.5 \cdot 10^{-5}$	$\text{s}^{-1}$
Maintenance coefficient	$m_S$	$3 \cdot 10^{-5}$	$3 \cdot 10^{-5}$	$\text{kgS kgX}^{-1} \text{s}^{-1}$
Oxygen saturation constant	$K_S$	$0.35 \cdot 10^{-3}$	$0.35 \cdot 10^{-3}$	$\text{kgX m}^{-3}$
Biomass yield on substrate	$Y_{XS}$	0.045	0.045	$\text{kgX kgS}^{-1}$
Maximum biofilm biomass density	$C_{Xm}$	70	70 and 7	$\text{kgX m}^{-3}$
Oxygen diffusion coefficient	$D$	$1.6 \cdot 10^{-9}$	$2 \cdot 10^{-9}$	$\text{m}^2 \text{s}^{-1}$
Liquid kinematic viscosity	$\nu$	-	$10^{-6}$	$\text{m}^2 \text{s}^{-1}$
Liquid density	$\rho$	-	1000	$\text{kg m}^{-3}$
Maximum liquid velocity in input	$u_{X,max}$	-	0.001, 0.004 and 0.01	$\text{m s}^{-1}$
Concentration boundary layer thickness	$\delta$	$40 \cdot 10^{-6}$	calculated	$\text{m}$
Number of grid elements inoculated	$n_0$	1000 on plate 20 on sphere	5 and 15	-

### Diffusion, reaction and growth model

#### Growth of biofilms on planar surfaces

DRG simplification of the general model assumes that the substrate coming from the bulk liquid diffuses through the CBL and biofilm matrix and it is consumed by the bacteria which use it for growth (Picioreanu *et al.*, 1998b). The concentration boundary layer is parallel to the carrier surface, it has a constant thickness in time, and it moves upwards as the biofilm thickness increases. Although these assumptions seem trivial, they still can be a realistic approximation for a system with a very slow liquid flow over the biofilm (see the oxygen microelectrode measurements by de Beer and Stoodley, 1995).

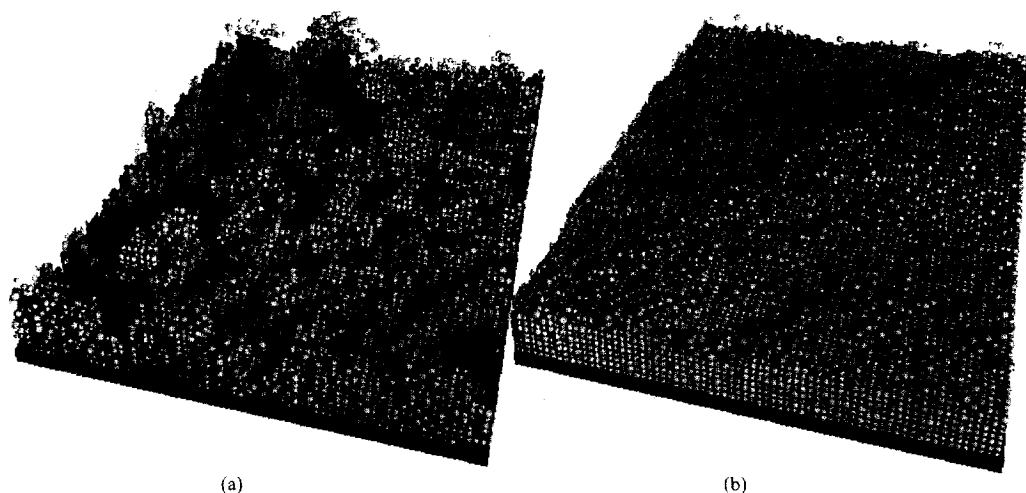


Figure 3. Three-dimensional simulations of biofilm development on a planar surface in (a) substrate transfer limited regime after 10 days; (b) biomass growth limited regime after 2 days. The biomass concentration at each grid node is proportional to the size of the particles used in this 3-D visualisation.

The results of such 3-D models (Picioreanu *et al.*, 1998b) suggest that in a mass transfer limited regime the biofilm develops as a heterogeneous structure, presenting pores, channels and “mushroom”-like bacterial clusters (Figure 3a), whereas in a substrate non-limited regime a compact, and densely-packed biofilm forms (figure 3b). The (non-quantitative) models of Wimpenny and Colasanti (1997) and Hermanowicz (1998) show the same trend. Biofilm morphology can however, be quantified by measures as surface roughness ( $\sigma$ ), surface area enlargement ( $A_f$ ), fractal dimension of the surface ( $F$ ), biofilm compactness ( $C_p$ ) or porosity ( $\epsilon$ ) defined in Picioreanu *et al.* (1998b). By plotting these measures against the ratio between maximum biomass growth rate and maximum substrate transport rate ( $G$ ), the effect of different growth regimes on biofilm structure can be clearly seen (Figure 4).

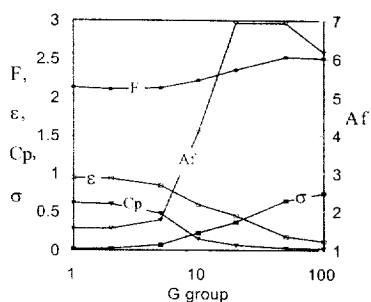


Figure 4. Influence of biomass growth rate/substrate transport rate ratio ( $G$  group) on some biofilm characteristics.

#### Growth of biofilms on spherical carriers

One of the advantages of a discrete approach is that, once the model equations have been developed, the boundary conditions and the geometry of the system can be easily changed. The carrier surface, for instance, can be spherical (Figure 5) instead of flat. One can model in this way the development of biofilms in particle reactors (fluidized bed, airlift, etc.).

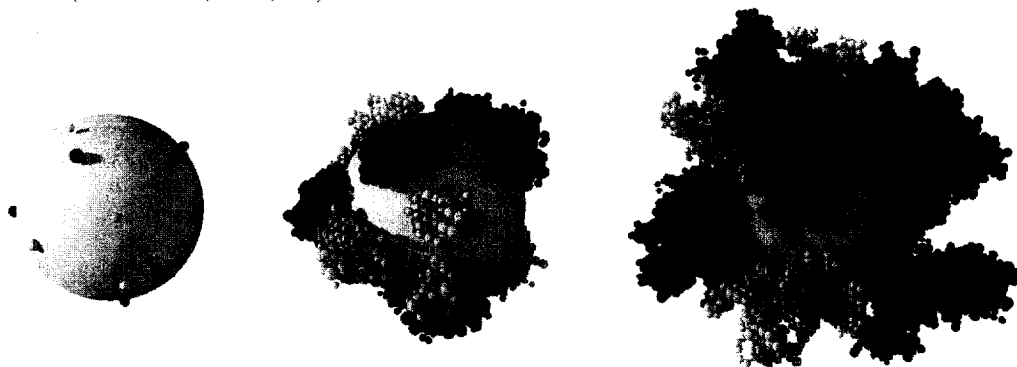


Figure 5. Simulated evolution in time of a two-species biofilm grown on a spherical carrier (mass transfer limited regime). The biomass concentration at each grid node is proportional to the size of the particles used in this 3-D visualisation.

#### Convection, diffusion, reaction and growth model

##### Growth of biofilms on planar surfaces

The two-dimensional CGRG model was used to investigate the role of different environmental conditions on the biofilm evolution. It has been found that several dimensionless parameters currently used in chemical and biochemical engineering, e.g. the Reynolds number  $Re = u_{x,\max} L_y / \nu$ , Schmidt number  $Sc = \nu / D$ ,

Thiele number  $\phi^2 = L_y^2 \frac{(\mu_m / Y_{XS} + m_s) C_{Xm}}{D_s C_{S0}}$ , Monod saturation constant  $K = K_s / C_{S0}$  can significantly affect the biofilm development. The number ( $n_0$ ) and initial distribution of microorganisms on the carrier surface is also of importance for further biofilm formation.

At high  $Re$  numbers the external resistance to mass transfer diminishes by decreasing the thickness of both hydrodynamic and concentration boundary layers (Figure 6a,b,c). This has the effect of smoothing the biofilm surface. Conversely, at lower  $Re$  (i.e., low fluid velocities) the thickness of CBL increases producing a rough biofilm. Pores and channels form in the biofilm as a result of nutrient depletion between the different bacterial colonies. Due to the steep gradient of substrate concentration, the biofilm top layer will grow much faster than the bottom layer giving a finger-like shaped biofilm.

The internal resistance to mass transfer, characterised by the Thiele number  $\phi^2$ , influences in the same way the biofilm formation. High  $\phi^2$  (given by a high specific substrate consumption rate, high biomass concentration  $C_{Xm}$ , low substrate diffusivity in the biofilm  $D$ , or low substrate concentration in the liquid  $C_{S0}$ ) make the biofilm structure more heterogeneous (figure 6a,b,c,d). At low  $\phi^2$  (high internal substrate transfer rate) the resulting structure is more compact and homogeneous (Figure 6e,f) because the substrate penetrates deeper into the biofilm.

At a small number of initially attached cells ( $n_0$ ), the biofilm is made of big colonies separated by large and deep channels. When the carrier surface is densely populated at the initial stages, a rough biofilm with narrow channels will develop. By comparing the position of inoculum cells on the substratum with the actual colony spreading, we can see from figures 6 that the bacterial colonies naturally extend in the direction of maximum substrate availability (to the left side and upwards, in this case). There is therefore no need to introduce an *explicit* microscopic rule for a preferential direction of bacterial division.

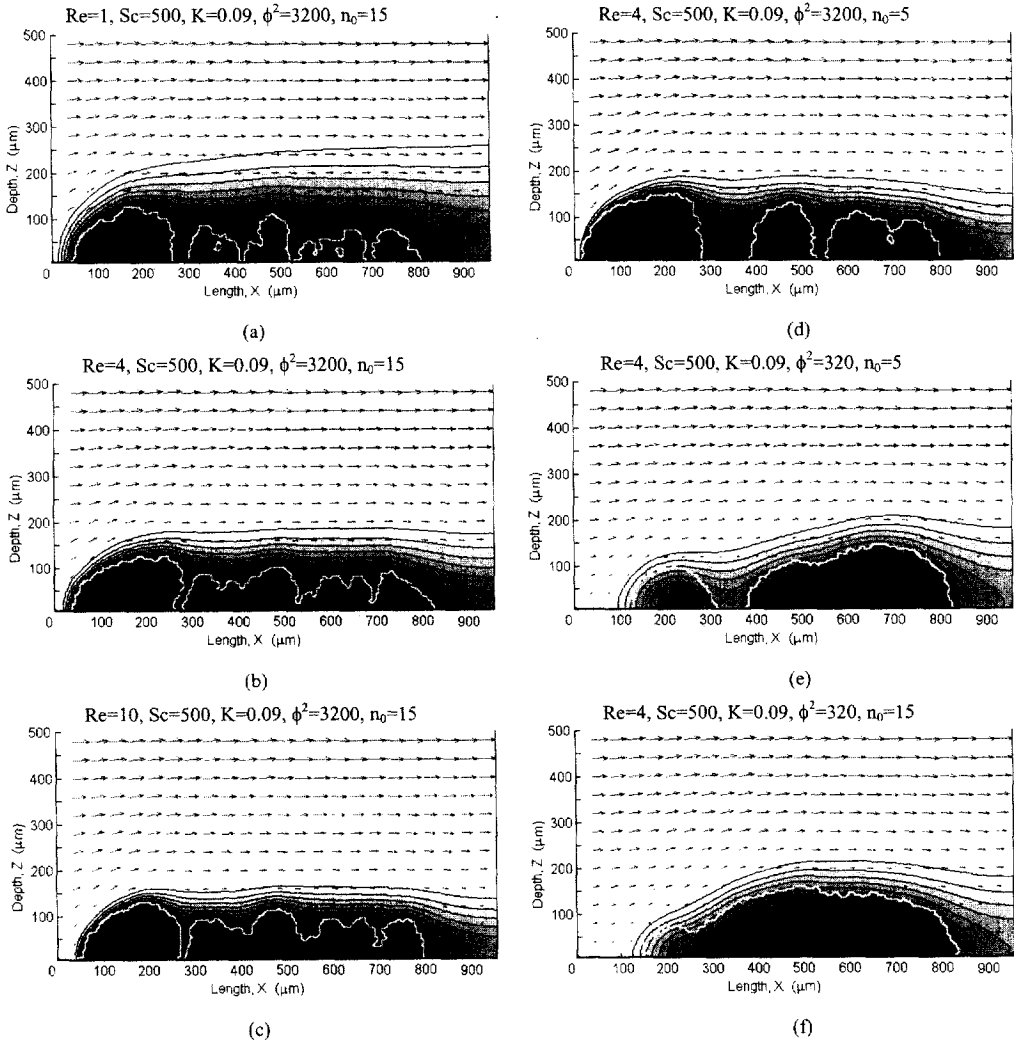


Figure 6. Two-dimensional simulations of biofilm development under flow conditions: biofilm state after (a) 14 days; (b), (d) 10 days; (c) 9 days and (e), (f) 3 days. The biofilm surface is shown by a thick white line. The arrows represent the averaged value of vector velocity on a  $8 \times 8$  square of grid nodes. Black lines indicate iso-concentration contours of substrate (10% increment between lines) from the maximum value in the bulk liquid (white region) to the areas depleted in substrate (dark grey regions). The black spots show the position of inoculum cells.

## CONCLUSIONS

A good fully quantitative model approach has been developed. The multidimensional model includes biofilm processes such as fluid flow over irregular biofilm surface, substrate transport by convection and diffusion, substrate consumption and biomass growth. Incorporation of biofilm detachment is being studied at the moment. Moreover, the physical, chemical and biological parameters widely known (as reaction rate constants, diffusivities, component concentrations and fluid velocities) can be directly used in the model.

System geometry can be easily modified by changing the boundary conditions. The model can cope with any arbitrary substratum shape. It can also be easily adapted to represent multispecies and multisubstrate biofilm systems, making it a very useful tool to study biofilm ecology issues.

Different biofilm structures are generated by this model, ranging from compact structures to porous and channelled ones. The results support a previously postulated mechanism for biofilm structures (van Loosdrecht *et al.*, 1995). A heterogeneous biofilm with rough surface and high porosity occurs in the slow substrate transfer regime, which is generated either by slow flow (high external mass transfer resistance) or by small substrate diffusivity in the biofilm (high internal resistance to mass transfer). In a substrate non-limited case generated by fast flow and fast internal diffusion, the biofilm develops as a compact structure.

## ACKNOWLEDGEMENTS

This research is funded by the *Netherlands Organisation for Applied Scientific Research* (TNO) by the contract 95/638/MEP.

## REFERENCES

- de Beer, D., Stoodley, P., Roe, F. and Lewandowski, Z. (1994). Effects of biofilm structures on oxygen distribution and mass transport. *Biotechnol. Bioeng.* **43**, 1131-1138.
- de Beer, D. and Stoodley, P. (1995). Relation between the structure of an aerobic biofilm and transport phenomena. *Wat. Sci. Tech.* **32**(8), 11-18.
- Bishop, P. and Rittmann, B. E. (1996). Modelling heterogeneity in biofilms: Report of the discussion session. *Wat. Sci. Tech.* **32**(8), 263-265.
- Chen, S., Dawson, S. P., Doolen, G. D., Janecky, D. R. and Lawniczak, A. (1995). Lattice methods and their applications to reacting systems. *Computers Chem. Engng.* **19**(6/7), 617-646.
- Chen, Y., Ohashi, H. and Akiyama, M. (1997). Simulation of laminar flow over a backward-facing step using the lattice BGK method. *JSME Int. J., Series B*, **40**(1), 25-32.
- Gjaltema, A., Arts, P. A. M., van Loosdrecht, M. C. M., Kuennen, J. G. and Heijnen, J. J. (1994). Heterogeneity of biofilms in rotating annular reactors: Occurrence, structure and consequences. *Biotechnol. Bioeng.*, **44**, 194-204.
- Hermanowicz, S. W. (1998). A model of two-dimensional biofilm morphology. *Wat. Sci. Tech.*, **37**(4-5), 219-222.
- Kugaprasatham, S., Nagaoka, H. and Ohgaki, S. (1992). Effect of turbulence on nitrifying biofilms at non-limiting substrate conditions. *Wat. Res.*, **26**(12), 1629-1638.
- Kwok, W. K., Picioreanu, C., Ong, S. L., van Loosdrecht, M. C. M., Ng, W. J. and Heijnen, J. J. (1998). Influence of biomass production and detachment forces on biofilm structures in a biofilm airlift suspension reactor. *Biotechnol. Bioeng.* **58**(4), 400-407.
- Picioreanu, C. (1996). Modelling biofilms with cellular automata. Final report to *European Environmental Research Organisation*, April 1996, Wageningen, The Netherlands.
- Picioreanu, C., van Loosdrecht, M. C. M. and Heijnen, J. J. (1998a). A new combined differential-discrete cellular automaton approach for biofilm modeling: Application for growth in gel beads. *Biotechnol. Bioeng.*, **57**(6), 718-731.
- Picioreanu, C., van Loosdrecht, M. C. M. and Heijnen, J. J. (1998b). Mathematical modeling of biofilm structure with a hybrid differential-discrete cellular automaton approach. *Biotechnol. Bioeng.*, **58**(1), 101-116.
- Ponce Dawson, S., Chen, S. and Doolen, G. D. (1993). Lattice Boltzmann computations for reaction-diffusion equations. *J. Chem. Phys.* **98**(2), 1514-1523.
- Rittmann, B. E. and Manem, J. A. (1992). Development and experimental evaluation of a steady-state, multispecies biofilm model. *Biotechnol. Bioeng.*, **39**, 914-922.
- Van Loosdrecht, M. C. M., Eikelboom, D., Gjaltema, A., Mulder, A., Tjihuis, L. and Heijnen, J. J. (1995). Biofilm structures. *Wat. Sci. Tech.* **32**(8), 235-243.
- Wanner, O. and Gujer, W. (1986). Multispecies biofilm model. *Biotechnol. Bioeng.*, **28**, 314-328.
- Wentland, E. J., Stewart, P., Ching-Tsan, H. and McFeters, G. A. (1996). Spatial variations in growth rate within *Klebsiella pneumoniae* colonies and biofilm. *Biotechnol. Prog.*, **12**, 316-321.
- Wimpenny, J. W. T. and Colasanti, R. (1997). A unifying hypothesis for the structure of microbial biofilms based on cellular automaton models. *FEMS Microb. Ecol.*, **22**, 1-16.